Available online at www.sciencedirect.com

Catalysis Today 96 (2004) 211–222

www.elsevier.com/locate/cattod

Designing the activity/selectivity of surface acidic, basic and redox active sites in the supported $K_2O–V_2O_5/Al_2O_3$ catalytic system

Xiang Wang, Israel. E. Wachs*

Operando Molecular Spectroscopy and Catalysis Laboratory, Department of Chemical Engineering, Lehigh University, Bethlehem, PA 18015 ,USA

Abstract

The supported $K_2O–V_2O_5/Al_2O_3$ catalytic system was designed to create surfaces that were 100% acidic, 100% basic, 100% redox, mixed redox-acidic and mixed redox-basic. The resulting nature of the surface sites was controlled by the impregnation of the specific additives (K-basic or V-redox/acidic), their order of impregnation and their surface coverage. The exact locations of the surface methoxy intermediates ($Al–OCH_3$, $K–OCH_3$ or $V–OCH_3$) on the mixed oxide catalyst surfaces during methanol oxidation were determined with in situ Raman spectroscopy. The surface chemistry of the various surface sites and their surface reaction intermediates were chemically probed by CH_3OH oxidation steady-state and temperature programmed surface reaction (TPSR) spectroscopy studies. The specific reactivity order and the product selectivity of the various surface sites were found to be: $V–OCH_3$ (HCHO) $\sim$ $Al–OCH_3$ (CH_3OCH_3) $\gg$ $K–OCH_3$ (primarily CO_2 and minor amounts of HCHO). Formation of dimethoxy methane, $(CH_3O)_2CH_2$, required the presence of dual surface redox-acidic sites surface redox sites to yield H_2CO and surface acidic sites to insert the surface methoxy into H_2CO to form dimethoxy methane, $(CH_3O)_2CH_2$. The addition of basic surface potassium oxide to Al_2O_3 possessing surface acid sites completely suppressed reactions from the surface acidic sites and formed a surface with only basic characteristics. The addition of redox surface vanadia to the supported K_2O/Al_2O_3 catalyst was able to completely suppress reactions from surface basic sites and formed a surface with only redox characteristics. These studies demonstrate that it is possible to determine the specific surface site requirements for each reaction pathway for methanol oxidation to products, and that this informative approach should also be applicable to other reactant molecules.

Keywords: Supported metal oxide catalyst; Al_2O_3; V_2O_5; Potassium oxide (K_2O); Methanol oxidation; Formaldehyde, dimethyl ether, dimethoxy methane; Carbon dioxide; Characterization; BET; In situ Raman spectroscopy; Temperature programmed surface reaction (TPSR) spectroscopy

1. Introduction

Supported vanadium oxide catalysts are well-known for their efficiency in selective oxidation reactions and are widely used in many industrial processes such as selective catalytic reduction (SCR) of NO*x* with NH_3 [1], sulphur dioxide oxidation [2], oxidation of *o*-xylene to phthalic anhydride [3,4], hydrocarbon oxidative dehydrogenation [5–7] and ammoxidation of alkyl aromatics to nitriles [8]. In addition, supported vanadia catalysts have also been examined for many other reactions such as methanol oxidation and partial oxidation of hydrocarbons for the purpose of obtaining fundamental catalytic insights [9–14]. The catalytic performance of supported vanadia catalysts can also be greatly modified by the introduction of additives that affect the activity and selectivity, thus, achieving catalysts with high specificity for the targeted reaction products [1,2,9–14].

The addition of basic potassium oxide to supported vanadia catalysts is known to influence the activity of the surface vanadia species by retarding its redox potential and simultaneously increasing its selectivity in oxidation reactions [9–14]. The order of impregnation of potassium oxide and vanadia is also known to have an effect on the resulting catalytic properties [9–14]. Surface potassium

---

* Corresponding author. Tel.: +1 610 758 4274; fax: +1 610 758 6555.
E-mail address: iew0@lehigh.edu (Israel. E. Wachs).

0920-5861/$ – see front matter © 2004 Elsevier B.V. All rights reserved.
doi:10.1016/j.cattod.2004.06.145

oxide coordinates to the surface vanadia species, reduces the terminal V=O bond order, decreases the number of active surface acidic sites and increases the number of surface basic sites [9–14]. Thus, the supported V_2O_5–K_2O/Al_2O_3 catalysts represent an interesting system to further investigate how to design model metal oxide surfaces with specific active surface sites (redox, acidic, basic, redox-acidic and redox-basic).

In the present study, the effects of basic potassium oxide on the nature of the active surface sites of supported V_2O_5/Al_2O_3 and Al_2O_3 catalysts were investigated by using the methanol oxidation chemical probe reaction. Additional fundamental insights into the surface structures, surface reaction intermediates and the surface reaction mechanisms were obtained from in situ Raman and temperature programmed surface reaction (TPSR) spectroscopy studies. Based on these results, the surface structure-reactivity/selectivity relationships have been determined for methanol oxidation over the supported K_2O–V_2O_5/Al_2O_3 catalytic system that allows for its design for specific reaction products (formaldehyde, dimethyl ether, dimethoxy methane or CO/CO_2).

2. Experimental

2.1. Catalyst preparation

The catalysts employed in this study were prepared by the incipient wetness impregnation method. The Al_2O_3 (Engelhard, 214 m^2/g) support was calcined in air at 500 °C for about 2 h before being used for the catalyst preparations. To achieve monolayer coverage of the two-dimensional surface vanadia species on the Al_2O_3 support, the vanadia loading was maintained around 20% V_2O_5 [9]. For the potassium oxide modified supported V_2O_5/Al_2O_3 samples, an 11.5% K_2O loading was used in order to maintain a K/V molar ratio of 1/1. In order to investigate the effect of preparation sequence on the properties of the catalysts modified by potassium oxide, two K_2O–V_2O_5/Al_2O_3 samples with an inverse K_2O and V_2O_5 addition sequence were prepared. The 11.5% K_2O/Al_2O_3 and 11.5% K_2O/20% V_2O_5/Al_2O_3 samples were prepared by the impregnation of an aqueous solution of KNO_3 (J. T. Baker, 99.7%) onto Al_2O_3 and 20% V_2O_5/Al_2O_3 supports, respectively. After impregnation, the samples were dried at room temperature overnight. The catalysts were subsequently calcined in air at 600 °C for 4 h to ensure that KNO_3 completely decomposed. The 20% V_2O_5/Al_2O_3 and 20% V_2O_5/11.5% K_2O/Al_2O_3 were prepared by the impregnation of an isopropanol solution of $VO(OC_3H_7)_3$ (Alfa Aesar, 95–99%) onto Al_2O_3 and 11.5% K_2O/Al_2O_3, respectively, in a glove box under a continuous N_2 flow. After impregnation, the samples were subsequently dried inside the glove box overnight in a N_2 flow at room temperature. The samples were subsequently calcined in air at 600 °C for 4 h.

2.2. BET specific surface area measurement

The specific surface areas of the samples were measured by nitrogen adsorption–desorption in flowing N_2 at 77 K with a QuantaChrome Sorption system. To better understand the change of the Al_2O_3 support specific surface area upon the addition of the various additives, the specific surface areas of Al_2O_3 in the different samples were also determined by assuming that the added vanadium and potassium oxides do not contribute to the surface area of the samples since they are essentially dispersed as two-dimensional metal oxide overlayers on the Al_2O_3 surface (confirmed with Raman spectroscopy) and that they only contribute to the mass of the sample.

2.3. In situ Raman spectroscopy

The in situ Raman spectra under flowing O_2/He and CH_3OH/O_2/He environments were obtained with the 514.5 nm line of an Ar^+ ion laser (Spectra Physics, Model 164). The scattered radiation from the sample was directed into a CCD detector (Jobin Yvon-Spex, ISA Inc., Model Spectrum-1) cooled with liquid N_2. The spectral acquisition consisted of 25 scans and 30 s per scan (12.5 min/spectrum). The samples were pressed into self-supported wafers loaded into an in situ quartz cell [15]. Afterwards, the in situ cell with the samples was heated to 450 °C and kept for ~1 h in a flowing O_2/He gas mixture (100 ml/min) containing ~20% O_2 to remove any possible combustible sample impurity. The samples were then cooled down to 230 °C, and the in situ Raman spectra of the dehydrated samples were collected. Subsequently, the methanol/O_2/He gas mixture flow (100 ml/min) was introduced into the in situ Raman cell with a CH_3OH/O_2/He molar ratio of 4/20/76 at 230 °C and the in situ Raman spectra were collected after ~30 min to allow steady state conditions to be reached.

2.4. CH_3OH-temperature programmed surface reaction spectroscopy

Methanol-TPSR was performed on a Zeton-Altamira temperature programmed system (AMI-100) equipped with an online quadrupole mass spectrometer (Dycor Dymaxion DME200MS). The samples, ~40 mg, were loaded into a U-shaped quartz tube and initially calcined at 450 °C (Ultra Zero Grade O_2/He, 30 ml/min) for ~1 h to remove any possible adsorbed impurities. To ensure that the supported vanadium species on the catalysts remain in a fully oxidized state, the pretreated samples were first cooled down in flowing air to110 °C and then the gas stream was switched to an ultra high purity He flow upon further cooling to 100 °C. After flushing with continuously flowing He for another 1 h at 100 °C to remove any physically adsorbed oxygen or potential background gases, a CH_3OH/He gas mixture feed (30 ml/min) containing 2000 ppm methanol was introduced for chemisoprtion and maintained for

~30 min. Previous work demonstrated that the adsorption temperature of 100 °C can minimize the formation of physically adsorbed methanol on the samples since the CH_3OH desorption temperature is below this temperature [16,17]. After methanol adsorption, the samples were purged again at 100 °C with a He flow for an additional 1 h to remove any residual physically adsorbed methanol. The TPSR experiments were then performed with a heating rate of 10 °C/min in an UHP He flow, with the signals monitored by the online MS. The *m*/*e* values used to detect the different desorption products were $m/e = 31$ for CH_3OH, $m/e = 30$ for H_2CO, $m/e = 45$ for CH_3OCH_3 (DME), $m/e = 76$ for $(CH_3O)_2CH_2$ (DMM), $m/e = 44$ for CO_2 and $m/e = 28$ for CO. For desorbing products that gave rise to several fragments in the mass spectrometer, additional *m*/*e* values were also collected to confirm the identity of the desorbing products (e.g., $m/e = 45$ for $CH_3OCH_3^+$ and $m/e = 15$ for the assicated CH_3^+ cracking fragment).

The kinetics of the surface methoxy reactions can be determined from the TPSR heating rate, 10 °C/min, and the assumption that the first-order pre-exponential factor is $10^{13}\ s^{-1}$, a typical observed pre-exponential factor for surface methoxy reactions [16], by use of the Redhead equation for first-order kinetics:

$$\frac{E_{act}}{RT_p^2} = \frac{\nu}{\beta}\exp\left(-\frac{E_{act}}{RT_p}\right) \tag{1}$$

where T_p is the TPSR peak temperature, $\nu = 10^{13}\ s^{-1}$ and $\beta = 0.17$ °C/s. This equation can be applied to these supported vanadia catalysts without any corrections for re-adsorption since recent TPSR studies by Vohs et al. demonstrated that the same T_p temperatures are obtained with single crystals and powders for the methanol partial oxidation products that are not over-oxidized by re-adsorption [16]. Unlike single crystal studies in vacuum, it is not possible to determine or relate the kinetic parameters from the FWHM of the TPSR curve since the desorbing products signals becomes broadened due to dispersion of the gases as they pass through the thin catalyst bed. Consequently, only the T_p temperature during CH_3OH-TPSR can be accurately determined.

2.5. Steady-state methanol oxidation

Steady-state methanol oxidation was used to chemically probe the nature of the active surface sites of the catalysts. The reaction was performed in an isothermal fixed-bed differential reactor at atmospheric pressure. The amount of catalyst varied from 25 to 100 mg, depending on the specific activity of the catalyst. The volume composition of the gaseous reactant feed was 6% CH_3OH, 13% O_2 and balance He, with the total flow rate of ~100 ml/min. To maintain differential reaction conditions, the methanol conversion was always maintained below 10% by varying the amount of catalyst sample in the reactor. The specific CH_3OH conversions obtained at 230 °C for the different catalysts were 7.2% for Al_2O_3, 3.4% for 11.5% K_2O/Al_2O_3, 9.0% for 20% V_2O_5/Al_2O_3, 2.5% for 11.5% K_2O/20% V_2O_5/Al_2O_3 and 7.8% for 20%V_2O_5/11.5% K_2O/Al_2O_3. The methanol conversion and reaction products were analyzed using an online gas chromatograph (HP 5890 series II) equipped with TCD and FID detectors. A Carboxene-1000 packed column and a CP-sil 5CB capillary column were used in parallel for TCD and FID, respectively.

3. Results

3.1. BET specific surface area

The specific surface areas of the samples are listed in Table 1. Compared with the Al_2O_3 support, all of the samples have lower surface areas primarily due to the added mass of vanadium and potassium oxides. To better understand the effect of the added vanadium and potassium oxides on the Al_2O_3 support surface area, the specific surface areas of the Al_2O_3 support of the different samples were also calculated. The specific surface areas of the Al_2O_3 support for 20% V_2O_5/Al_2O_3 and 11.5% K_2O/20% V_2O_5/Al_2O_3 are essentially unaltered, indicating that the direct contact of the surface vanadia species with the Al_2O_3 support does not change the Al_2O_3 surface area. However, direct contact of surface potassium oxide species with the Al_2O_3 support does somewhat decrease the specific surface area of the Al_2O_3 support, 14–19 %, for the 11.5% K_2O/Al_2O_3 and 20% V_2O_5/11.5% K_2O/Al_2O_3 catalysts.

3.2. In situ Raman spectroscopy

The molecular structure of the supported vanadia species and the modifying effects of the surface potassium oxide additive were investigated by in situ Raman spectroscopy. The Raman spectra of the dehydrated samples at 230 °C in an O_2/He flow are presented in Fig. 1. No Raman bands were observed for the Al_2O_3 support and supported 11.5% K_2O/Al_2O_3, which is consistent with other studies of such high surface area alumina supports [18]. The Raman spectrum of dehydrated 20% V_2O_5/Al_2O_3 exhibits two bands at 1021 and 931 cm^{-1} and no Raman bands due to crystalline V_2O_5 (994, 686 and 520 cm^{-1}) [18]. The strongest band at ~1021 cm^{-1}

Table 1
Specific surface areas (Ss) of catalysts

Catalysts	Ss of the samples	Ss of the Al_2O_3 in the samples
Al_2O_3	214	214
11.5% K_2O/Al_2O_3	163	184
20% V_2O_5/Al_2O_3	173	216
11.5% K_2O/20% V_2O_5/Al_2O_3	149	217
20% V_2O_5/11.5% K_2O /Al_2O_3	118	173

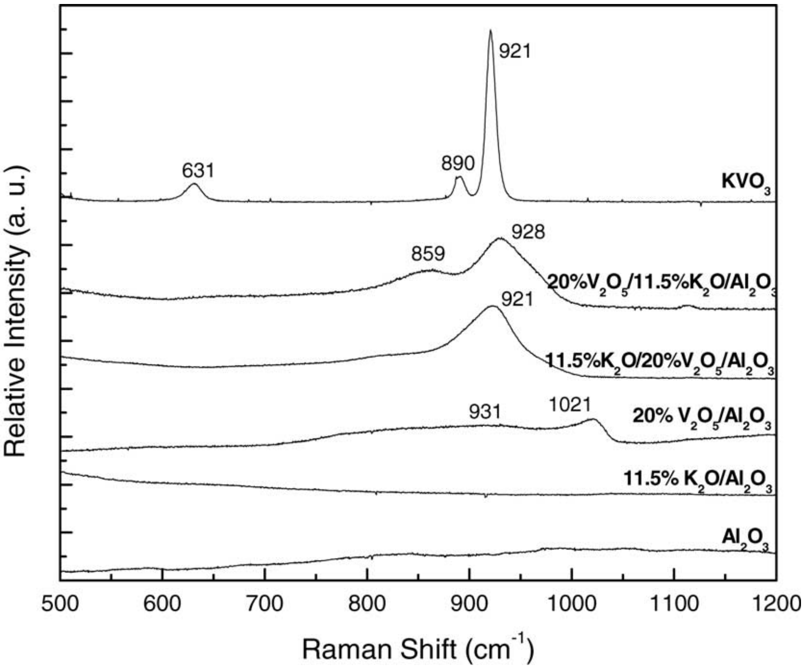

Fig. 1. In situ Raman spectra in the M–O stretching region in flowing O$_2$/He at 230 °C.

has been previously assigned to the dehydrated surface vanadate species possessing one terminal V=O bond and three bridging V–O–M bonds, where M is either an Al support cation or another surface V atom [18]. The broad Raman band at ~931 cm^{-1} is the characteristics of the symmetric stretch of either the bridging V–O–V or V–O–Al bond of the dehydrated polymeric surface vanadate species [18].

The Raman spectrum of dehydrated 20% V$_2$O$_5$/11.5% K$_2$O/Al$_2$O$_3$ shows two new Raman bands weak and strong bands at 859 and 928 cm^{-1}, respectively. Upon hydration, the Raman bands for the 20% V$_2$O$_5$/11.5% K$_2$O/Al$_2$O$_3$ catalyst shift position and also become much broader (especially the 928 cm^{-1} band). These changes upon hydration/dehydration reveal that the Al$_2$O$_3$ supported VO$_x$–KO$_x$ complexes are present as a two-dimensional monolayer on the Al$_2$O$_3$ support [18]. This suggests that the Raman bands at 859 and 928 cm^{-1} originate from the dehydrated surface VO$_x$ species that are significantly modified by the surface KO$_x$ species [14]. In contrast, the Raman band at 921 cm^{-1} for the dehydrated 11.5% K$_2$O/20% V$_2$O$_5$/Al$_2$O$_3$ catalyst does not shift position or become broader upon dehydration. This suggests that this band originates from a crystalline phase and not a surface metal oxide species [18]. The Raman band for the supported 11.5% K$_2$O/20% V$_2$O$_5$/Al$_2$O$_3$ at 921 cm^{-1} exactly matches that for bulk KVO$_3$, see Fig. 1, and demonstrates that the crystalline phase in this supported catalyst is KVO$_3$ [14]. It is also worth noting that since crystallites generally give much stronger Raman signals than the surface metal oxide species (typically by a factor of 10^1–10^2) [18], the KVO$_3$ crystallites only represent a minor fraction of the total vanadia present in the sample and that most of the vanadia is present as two-dimensional surface vanadia species.

In situ Raman spectroscopy was also used to monitor the formation of surface methoxy groups during the methanol oxidation reaction, which are the surface reaction intermediates for methanol oxidation (see Fig. 2). On the Al$_2$O$_3$ support, two weak Raman bands at 2835 and 2936 cm^{-1} are observed, which correspond to the stretching of the C–H bonds of the surface Al–OCH$_3$ species [15]. The two strong Raman bands on the supported 11.5% K$_2$O/Al$_2$O$_3$ for the surface K–OCH$_3$ intermediate shift to 2800 and 2926 cm^{-1}, respectively. The strong K–OCH$_3$ Raman bands preclude any conclusions about the presence of surface Al–OCH$_3$ because of its much weaker Raman band. Although no surface V–OCH$_3$ Raman bands are present for the supported 20% V$_2$O$_5$/Al$_2$O$_3$ catalyst, previous in situ IR and Raman studies indicate that a large amount of surface V–OCH$_3$ is indeed present during methanol oxidation but is not Raman active [15]. The origin of this unusual Raman/IR phenomenon is general for all V-alkoxides is currently not understood and is being further investigated. The main V–OCH$_3$ IR bands for supported 20% V$_2$O$_5$/Al$_2$O$_3$ catalyst are found at 2831 and 2931 cm^{-1} [15]. Although the loading of K$_2$O in the supported 11.5% K$_2$O/20% V$_2$O$_5$/Al$_2$O$_3$ is the same as in the supported 11.5% K$_2$O/Al$_2$O$_3$ catalyst, only two weak K–OCH$_3$ bands at 2807 and 2923 cm^{-1} are present for the former and no surface K–OCH$_3$ bands are observed for the latter. These in situ Raman spectra reveal that the surface methoxy intermediates on these two multi-component catalysts are primarily present as surface V–OCH$_3$ that are not Raman active, but IR active [15], since K–OCH$_3$ species give rise to strong Raman bands.

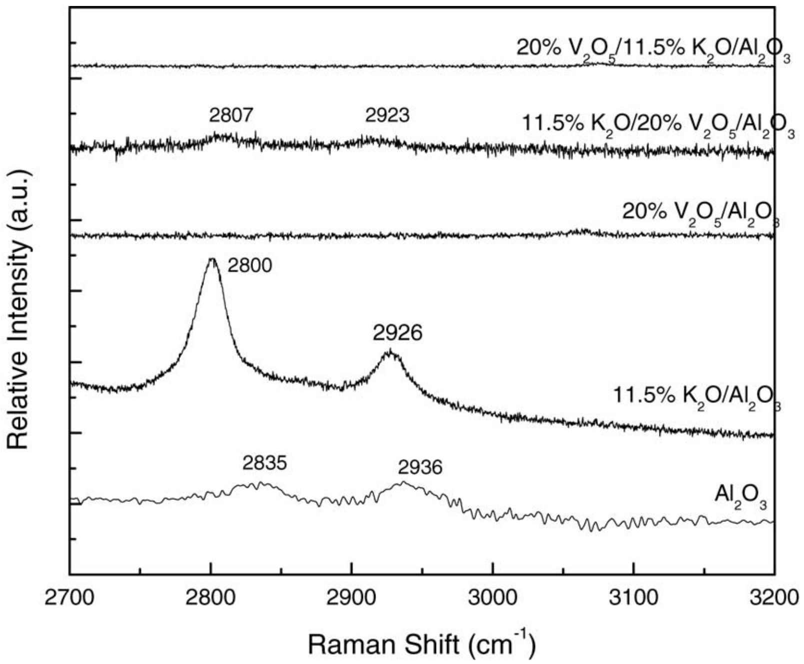

Fig. 2. In situ Raman spectra in the C–H stretching region in flowing $CH_3OH/O_2/He$ at 230 °C.

The absence of surface $V–OCH_3$ Raman bands actually allows the detection of weaker signals originating from surface $K–OCH_3$ or $Al–OCH_3$ species, but the latter was not observed in any of the alumina supported metal oxide catalysts indicating that surface Al^{3+} cations were not exposed.

3.3. CH_3OH-TPSR spectroscopy

CH_3OH-TPSR spectroscopy experiments with chemisorbed surface methoxy species were undertaken to chemically probe the reactivity and selectivity of the different surface methoxy intermediates formed on the supported $K_2O–V_2O_5/Al_2O_3$ catalysts. The CH_3OH-TPSR spectra for the different catalysts are presented in Fig. 3. Very different reaction products and reaction temperatures were observed for the different catalysts, indicating the presence of active surface sites possessing very different chemical activity and selectivity properties. The H_2O reaction product was always formed during the decomposition of the surface methoxy intermediates on all of the samples, but the H_2O formation curves are not included in the figures for simplicity since they do not add any additional insights. Another common feature of all of the samples is the formation of some CH_3OH, which originates from the self-hydrogenation of some surface methoxy intermediates from the surface H atoms formed during the decomposition of nearby surface methoxy intermediates [10,14,16,17]. Furthermore, CH_3OH formation from surface methoxy hydrogenation seems to mostly occur at the early stages of the formation of H_2CO and CH_3OCH_3 where the concentration of the surface methoxy species is most abundant.

The TPSR spectra for pure Al_2O_3 are presented in Fig. 3(a). A large quantity of DME, the characteristic product from surface acidic sites (surface Lewis sites are electron deficient as a result of oxygen vacancies present in transitional Al_2O_3), is the major product. The reaction of the surface $Al–OCH_3$ intermediates to yield DME initiates at ~125 °C with a T_p of ~190 °C. The addition of basic surface potassium oxide (surface basic sites are electron rich) onto the Al_2O_3 support, containing electron deficient sites, neutralized all of the surface Lewis acidic sites, as evidenced by the absence of DME that arise from surface acidic sites (see Fig. 3(b)). The predominant reaction product from the surface $K–OCH_3$ species is CO_2, which is accompanied by a small amount of HCHO and CH_3OH. Two CO_2 formation peaks are observed, with T_p values of ~255 and ~410 °C, with the former much broader than the latter. The presence of both CO_2 and H_2CO peaks, which appear simultaneously with respect to temperature, suggests that two different surface $K–OCH_3$ species are present for the surface potassium oxide layer on Al_2O_3. The higher surface $K–OCH_3$ decomposition temperatures relative to $Al–OCH_3$ reveal that surface $K–OCH_3$ intermediates are significantly less reactive than the surface $Al–OCH_3$ species. The main reaction product for the supported 20% V_2O_5/Al_2O_3 catalyst, shown in Fig. 3(c), is HCHO, reflecting that the surface of this catalyst possesses redox surface vanadia sites. Surface redox sites are able to give up an oxygen atom to a reducing reducing agent (e.g., $V^{5+}O_4 \rightarrow V^{3+}O_3$), such as methanol, and subsequently become oxidized by an oxygen carrier (e.g., $V^{3+}O_3 \rightarrow V^{5+}O_4$) such as O_2. The surface $V–OCH_3$ intermediates are also very active, as reflected by the low decomposition temperature of ~195 °C. Some DME is also formed for the supported V_2O_5/Al_2O_3 catalyst demonstrating the presence of a small amount of surface acidic sites in this sample. These surface acidic sites are not related to formation of Al–OCH_3 species since there are no exposed surface Al^{3+} cations and are related to the intrinsic acidity of the surface vanadia species on Al_2O_3, both surface Lewis acid sites containing oxygen vacancies and surface Bronsted acid sites containing H^+ [11,19].

These surface acidic sites are not present on the addition of potassium oxide for the supported 11.5% K_2O/20% V_2O_5/Al_2O_3 catalyst as reflected in the absence of DME formation during the TPSR experiment (see Fig. 3(d)). The only reaction products found on this catalyst are HCHO and CH_3OH, which are associated with the redox surface vanadia sites. Thus, the presence of surface potassium oxide increases the selectivity of the resultant catalyst towards the selective redox reaction. Two TPSR HCHO peaks are observed one at ∼195 °C and another at ∼255 °C. This indicates that two types of surface methoxy intermediates are formed on the supported 11.5% K_2O/20% V_2O_5/Al_2O_3 catalyst. The surface methoxy intermediate corresponding to the ∼195 °C peak is most probably corresponds to V–OCH_3 species formed on surface VO_x sites that were not influenced by K promoters since it possesses a similar temperature as

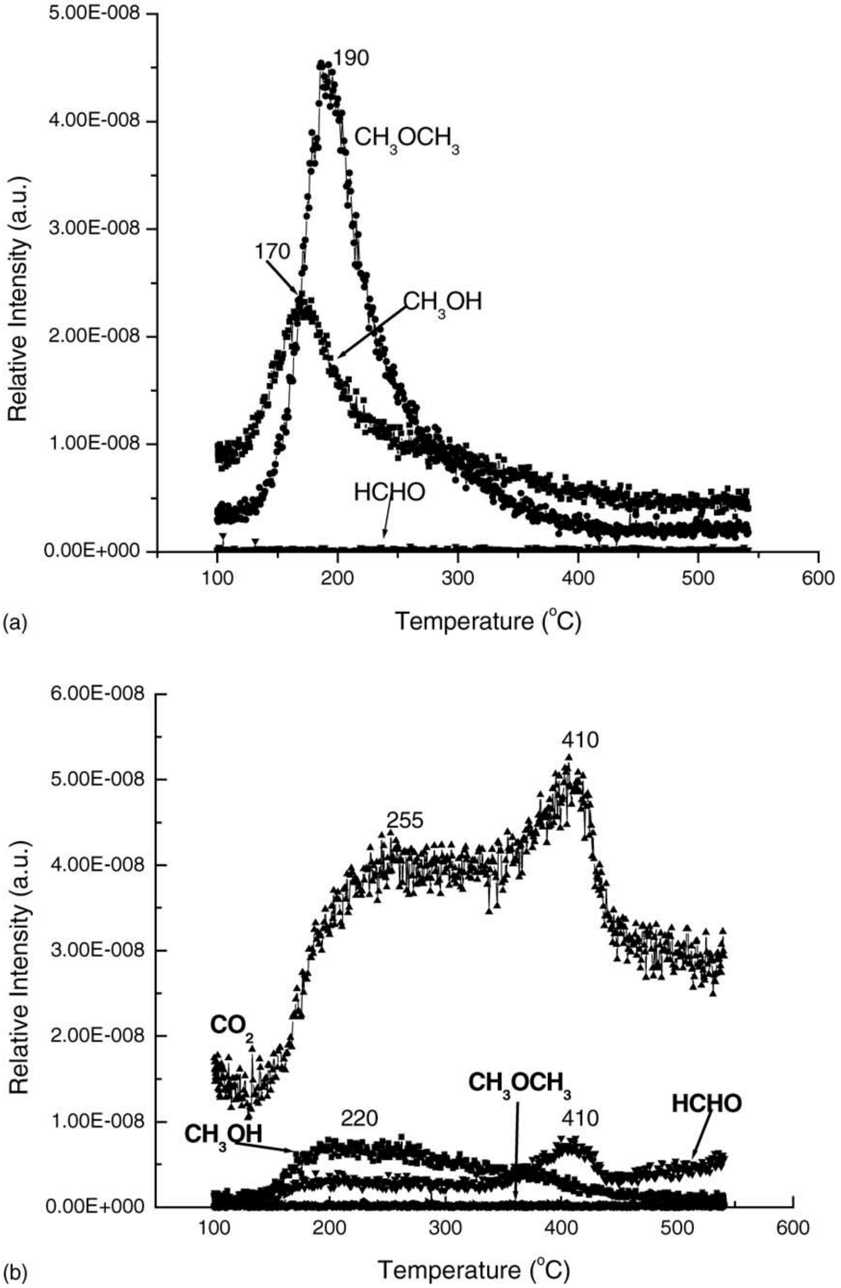

Fig. 3. CH_3OH-temperature programmed surface reaction (TPSR) spectra from: (a) Al_2O_3; (b) 11.5% K_2O/Al_2O_3; (c) 20% V_2O_5/Al_2O_3; (d) 11.5% K_2O/20% V_2O_5/Al_2O_3; (e) 20% V_2O_5/11.5% K_2O/Al2O_3.

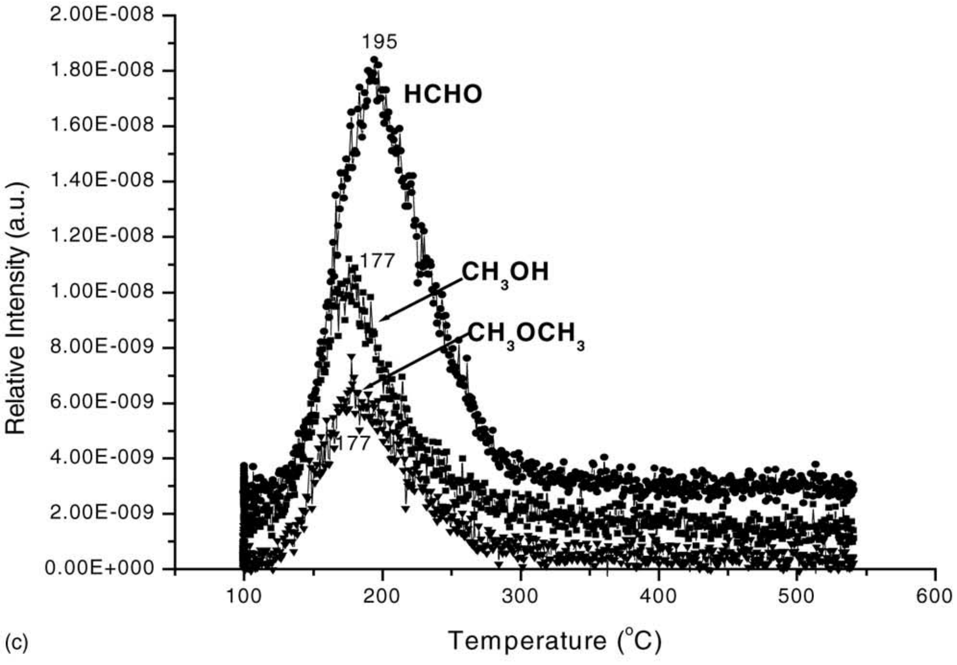

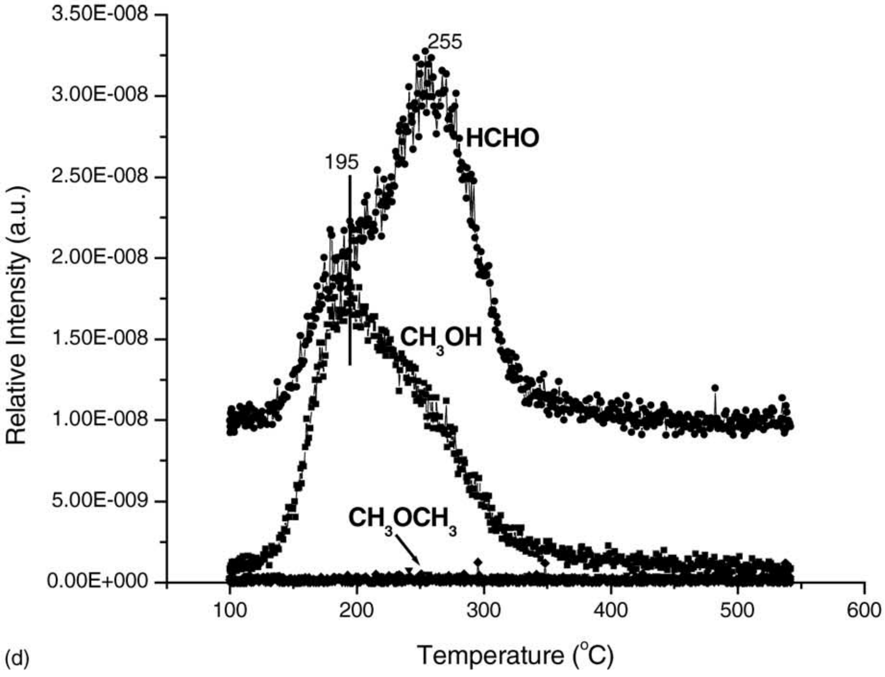

Fig. 3. (*Continued*)

the surface V–OCH_3 species observed for 20% V_2O_5/Al_2O_3 (~195 °C). However, the peak at ~255 °C most probably originates from surface V–OCH_3 species that have had their redox properties markedly retarded by coordination of surface potassium oxide (see in situ Raman spectra in Fig. 2). The in situ Raman results are consistent with this conclusion since only a very small amount of K–OCH_3 is detected for this sample (see Fig. 2).

The TPSR spectra of the supported 20% V_2O_5/11.5% K_2O/Al_2O_3 catalyst shown in Fig. 3(e) are surprisingly very different from that of the supported 11.5% K_2O/20% V_2O_5/Al_2O_3 catalyst as a consequence of changing the order of addition of vanadia and potassium oxide onto the Al_2O_3 support in the catalyst preparation. Surface acidic sites are suppressed as reflected by the absence of DME formation and H_2CO and CH_3OH reaction products appear as a sharp TPSR peak at 220 °C. The single and sharp TPSR peak suggests that only one type of surface methoxy intermediate is formed on this catalyst surface. However, the reactivity of the surface V–OCH_3 species has been affected by the surface

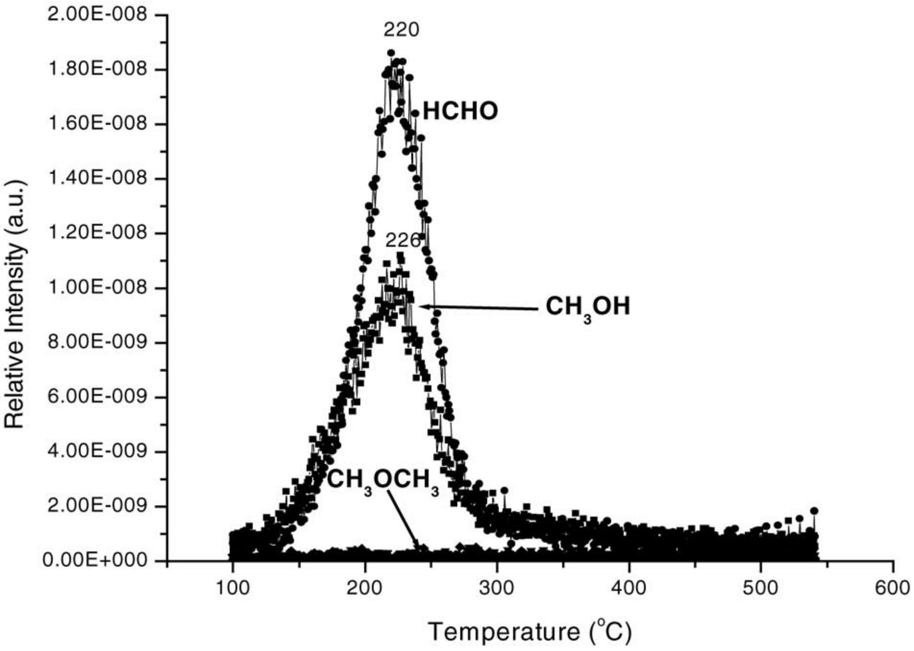

Fig. 3. (*Continued*).

potassium oxide on the Al_2O_3 support since the K-free supported 20% V_2O_5/Al_2O_3 catalyst exhibits a HCHO T_p that is ~25 °C lower than that for the catalyst prior to the addition of K_2O. Interestingly, the predominant surface V–OCH_3 reaction to form HCHO occurs at very different temperatures for supported 20% V_2O_5/11.5% K_2O/Al_2O_3 and for supported 11.5% K_2O/20% V_2O_5/Al_2O_3 (~220 and ~255 °C, respectively).

The surface methoxy TPSR peak temperatures, T_p, reaction products, ratio of H_2CO/CH_3OH, E_{act} and k_{rds} at 230 °C of the different catalysts were determined by application of the Redhead equation for first-order reaction kinetics (see CH_3OH-TPSR experimental section above for details) and are summarized in Table 2. It is interesting to observe that as the T_p of the surface V–OCH_3 species increased, due to the addition of the surface potassium oxide species, the ratio of H_2CO/CH_3OH decreased, which is consistent with the reduction in redox activity and, consequently, an increase in hydrogenation activity of the surface V–OCH_3 species. As the surface V–OCH_3 species became less active, higher T_p, the activation energy for the surface reactions increased and the first-order rate constants, k_{rds}, at 230 °C decreased by almost two orders of magnitude (see Table 2). The activation energy values increased when K_2O was added to the catalysts and this resulted in lower rate constants, k_{rds}, for the rate-determining step of the surface methoxy decomposition.

3.4. Steady-state methanol oxidation

Methanol oxidation was investigated over the different supported K_2O–V_2O_5/Al_2O_3 catalyst systems, under differential reaction conditions, and the results are presented in Table 3. The Al_2O_3 support contains only surface Lewis

Table 2
Surface methoxy decomposition temperatures and product distribution during CH_3OH-TPSR spectroscopy

Catalyst	Al_2O_3	11.5% K_2O/Al_2O_3		20% V_2O_5/Al_2O_3	11.5% K_2O/20% V_2O_5/Al_2O_3		20% V_2O_5/11.5% K_2O/Al_2O_3
Tp (°C)	190	255	410	195	195	255	220
Eact (Kcal/mol)	31.4	36.0	46.9	31.8	31.8	36.0	33.5
k_{rds} at 230 °C (s^{-1})	0.193	0.002	3.52×10^{-8}	0.136	0.136	0.002	0.024
K_{ads} (L/mol)	34	103	5.84×10^5	54	54	103	343
$A_{ads} \times 10^{-5}$ (L/mol)	36.2	1.1	0.1	38.5	38.5	1.1	44.4
ΔH_{ads} (Kcal/mol)	−11.4	−16	−26.9	−11.8	−11.8	−16	−13.5
Product distribution							
Major product	DME	CO_2		HCHO	HCHO		HCHO
Minor product	–	HCHO		DME	–		–
$HCHO/CH_3OH$ ratio (not calibrated)	–	0.4		2.1	1.2		1.4

Table 3
Steady state methanol oxidation on the catalysts

Catalyst	Ns (surface sites/nm^2)	Selectivity (%)				Rate (mmol/g h)	TOF (s^{-1}) × 10^{-3}
		HCHO	DMM	CO_2	DME		
Al_2O_3	3.4	–	–	–	100	121	9.5
11.5%K_2O/Al_2O_3	~8	30	–	70	–	2.8	0.3
20%V_2O_5/Al_2O_3	~8	50	40	–	10	85.8	10.8
11.5%K_2O/20%V_2O_5/Al_2O_3[a]	~8/8	85	–	15	–	2.3	0.3
20%V_2O_5/11.5%K_2O /Al_2O_3[b]	~8/8	100	–	–	–	95.0	12.0

Data were collected at 230 °C; $CH_3OH/O_2/He$ = 6/14/80.

[a] 20% V_2O_5/Al_2O_3 was prepared first, then KNO_3 was impregnated onto it.

[b] 11.5% K_2O/Al_2O_3 was prepared first, then $VO(OC_3H_7)_3$ was impregnated onto it.

acidic sites [19] that give rise to 100% DME selectivity, the characteristic methanol reaction product from surface acidic sites [20–22]. The addition of 11.5 wt.% K_2O onto the Al_2O_3 support completely suppresses the production of DME, indicating the neutralization of all of the surface acidic sites and the formation of a large quantity of CO_2, which reflects the presence of surface basic sites on this catalyst. The complete neutralization of the electron deficient Al_2O_3 surface acidic sites by the electron rich basic potassium oxide demonstrates that the supported 11.5% K_2O/Al_2O_3 catalyst must contain a two-dimensional monolayer of surface potassium oxide. HCHO was also formed as a minor reaction product over the supported 11.5% K_2O/Al_2O_3 catalyst with a selectivity of 30%, indicating that the basic surface potassium oxide species also possess surface redox character since the production of both H_2CO as well as CO_2 and H_2O require the consumption of oxygen.

Supported vanadia catalysts are well known for their redox properties and as partial oxidation catalysts. For the supported 20 wt.% V_2O_5/Al_2O_3 catalyst, large amounts of the partial oxidation products HCHO and DMM were formed from the surface redox sites, with a selectivity of 50 and 40%, respectively. Dimethoxy methane, $H_2C(OCH_3)_2$, is only formed at lower reaction temperatures due to the condensation of surface methoxy species at high surface intermediate coverage and the simultaneous presence of surface redox and acidic sites [21]. The surface acidic sites do not originate from surface Al–OCH_3 intermediates since in situ IR studies demonstrated that such species are not present when a two-dimensional surface vanadia monolayer is present [15]. These surface acidic sites are due to the presence of surface Lewis and Bronsted acidic sites associated with the surface vanadia monolayer itself [19].

Both supported 11.5% K_2O/20% V_2O_5/Al_2O_3 and 20% V_2O_5/11.5% K_2O/Al_2O_3 catalyst are highly selective towards HCHO with a selectivity of 85 and 100%, respectively. This suggests that the surface chemistry of these two multicomponent catalysts is dominated by surface vanadia redox species. For the supported 11.5% K_2O/20% V_2O_5/Al_2O_3 catalyst, 15% CO_2 is also produced indicating the presence of exposed surface potassium oxide basic sites. However, when vanadia was deposited after the potassium oxide on the Al_2O_3 supported, then no exposed surface basic sites appear to be present and only exposed surface redox sites are present in the supported 20% V_2O_5/11.5% K_2O/Al_2O_3 catalyst.

The catalytic activity is also a very important parameter to evaluate the performance of a given catalyst besides its selectivity to targeted reaction products since by definition selectivity is determined by the relative reaction rates. The reaction rates and turnover frequency (TOF) values for the different catalysts were determined and are listed in Table 3. The catalytic activities of the different samples, as well as their selectivity, are also dramatically modified by the presence of the various components on the Al_2O_3 support and by the different preparation orders. The Al_2O_3 support and the supported 20% V_2O_5/Al_2O_3 catalyst are very active with TOF values of $\sim 10 \times 10^{-3}\ s^{-1}$ at 230 °C. Their activities are significantly suppressed by the addition of potassium oxide, as evidenced by the significantly lower TOF values of $\sim 0.3 \times 10^{-3}\ s^{-1}$ at 230 °C for the supported 11.5% K_2O/Al_2O_3 and 11.5% K_2O/20% V_2O_5/Al_2O_3 catalysts. In contrast, although the supported 20% V_2O_5/11.5% K_2O/Al_2O_3 catalyst contains the same composition as the supported 11.5% K_2O/20% V_2O_5/Al_2O_3 catalyst, it still displays a high activity for the oxidation of methanol to formaldehyde. The comparable steady-state TOF values of the supported 20% V_2O_5/11.5% K_2O/Al_2O_3 and 20% V_2O_5/Al_2O_3 catalysts reveals that the activity of the 20% V_2O_5/11.5% K_2O/Al_2O_3 catalyst is not decreased by the presence of surface potassium oxide on the Al_2O_3 support. Thus, 100% redox selectivity is achieved in the supported 20% V_2O_5/11.5% K_2O/Al_2O_3 catalyst system by selectively poisoning the surface acidic sites by the basic surface potassium oxide and introducing very active redox surface vanadia sites that are orders of magnitude more active than the basic surface potassium oxide sites.

Combination of the methanol oxidation transient TSPR data and the steady-state kinetic data also allows for the quantitative determination of some of the thermodynamic adsorption properties (K_{ads}, ΔH_{ads} and A_{ads}) for methanol oxidation over these catalysts [9,23]:

$$\mathrm{TOF} = K_{ads} k_{rds} P_{CH_3OH} \tag{2}$$

$$E_{app} = E_{act} + \Delta H_{ads} \tag{3}$$

$$A_{\mathrm{app}} = \nu + A_{\mathrm{ads}} \tag{4}$$

$$k_{\mathrm{rds}} = \nu \exp\left(-\frac{E_{\mathrm{act}}}{RT}\right) \tag{5}$$

these kinetic parameters were defined in Eq. (1) above, and

$$K_{\mathrm{ads}} = A_{\mathrm{ads}} \exp\left(-\frac{\Delta H_{\mathrm{ads}}}{RT}\right) \tag{6}$$

where K_{ads} is the CH_3OH adsorption equilibrium constant, (H_{ads} is the heat of adsorption of CH_3OH on the catalyst surface (an exothermic process; larger negative values reflect stronger bonding of methanol to the catalyst surface) and A_{ads} is the adsorption pre-exponential factor. The apparent parameters E_{app} and A_{app} are composed of kinetic and thermodynamic terms as defined in Eqs. (3) and (4) above, respectively. The units for all of these kinetic and thermodynamic parameters are given in Table 2 as well as their quantitatively determined values from the CH_3OH-TPSR and steady-state methanol oxidation studies for each of the catalysts.

The addition of K_2O to the catalysts has a pronounced effect on the thermodynamic parameters for methanol oxidation as well as the kinetic parameters already presented earlier. Surface potassium oxide increases the exothermic surface heat of adsorption of methanol, which is reflected in the orders of magnitude increase of the methanol equilibrium adsorption constant, K_{ads}, and the affinity for methanol for these surfaces. There is also a concomitant decrease in the A_{ads} values, but the exponential term dominates the values of K_{ads}. It is also interesting that the H_2CO/CH_3OH integrated values from the CH_3OH-TPSR experiments reveal that the addition of surface potassium oxide to the supported V_2O_5/Al_2O_3 catalysts also increases the surface methoxy hydrogenation rate over the surface oxidative-dehydrogenation rate, which results in more CH_3OH being formed at the expense of H_2CO. Thus, the thermodynamic CH_3OH heat of adsorption has an influence on the selectivity of the H_2CO and CH_3OH reaction products during the CH_3OH-TPSR experiments.

Discussion

The in situ Raman studies during methanol oxidation provided direct fundamental information about the nature of the active surface sites and the surface reaction intermediates. Characterization of the various alumina-supported catalysts during methanol oxidation revealed that (1) the Al_2O_3 catalyst exclusively consisted of Al–OCH_3 surface species, (2) the 11.5% K_2O/Al_2O_3 catalyst exclusively consisted of a monolayer of surface KO_x species since only K–OCH_3 surface species and no exposed surface Al–OCH_3 sites were detected, and (3) the 20% V_2O_5/Al_2O_3 catalyst possessed a monolayer of surface vanadia species and exclusively consisted of V–OCH_3 surface species since surface Al–OCH_3 species were not detected. For the alumina-supported mixed metal oxide catalysts, the 20% V_2O_5/11.5% K_2O/Al_2O_3 catalyst consisted of a monolayer of surface V–OCH_3 species anchored to the 11.5% K_2O/Al_2O_3 substrate and the 11.5% $K_2O/V_2O_5/Al_2O_3$ catalyst consisted of a monolayer of surface V–OCH_3 and minor amounts of surface K–OCH_3 species and crystallites of KVO_3.

The CH_3OH-TPSR spectroscopy experiments provided additional insights into the nature of the surface active sites as well as their surface chemistry and kinetics. The acidic surface Al–OCH_3 complex exclusively yielded CH_3OCH_3 as the reaction product at modest temperatures. The acidic surface reaction mechanism proceeds via:

$$CH_3OH + * + O* \rightarrow CH_3O * + HO* \tag{7}$$

$$CH_3O^* + * \rightarrow CH_3^* + O* \quad \text{rds : rate determining step} \tag{8}$$

$$CH_3^* + CH_3O^* \leftrightarrow CH_3OCH_3 + 2^* \tag{9}$$

$$HO * + HO * \leftrightarrow H_2O + O* \tag{10}$$

where * denotes an active surface site, which is an Al site for Al_2O_3. The rate-determining-step (rds) is the slowest step in the above sequence of surface catalyzed elementary reaction steps and involves breaking one of the surface Al–OCH_3 C–O bonds to form the DME reaction product at ~190 °C. Kinetic isotopic experiments with CH_3OH and CD_3OD revealed that the rate of DME formation does not depend on breaking either the C–H or O–H bonds [24] and, consequently, only depends on breaking of the C–O bond of the surface methoxy intermediate (reaction step 10). Furthermore, the formation of DME proceeds by a Langmuir-Hinselwood reaction mechanism that does not involve gas-phase CH_3OH since the reaction readily takes place in the absence of gaseous CH_3OH during the CH_3OH-TPSR experiment in flowing He. The reversible dissociative chemisorption of methanol, reaction step 9, is reflected in the production of the CH_3OH reaction product at ~170 °C from surface methoxy species during CH_3OH-TPSR and the formation of CH_3OD and CD_3OH during transient isotope exchange experiments [24]. The reversible nature of reaction steps 11 and 12 is well documented in the literature [25–27]. Furthermore, both the in situ Raman and CH_3OH-TPSR spectra reveal that surface Al–OCH_3 species is the most abundant reaction intermediate (MARI).

The basic surface K–OCH_3 complex primarily produced CO_2 and minor amounts of H_2CO reaction products during the CH_3OH-TPSR experiment. Note that no DME was formed indicating that the basic surface KO_x species essentially titrated all the surface Lewis acidic sites of the Al_2O_3 support and that the surface KO_x was highly dispersed on the alumina substrate. The relatively higher temperatures for the formation of CO_2 at 255 and 410 °C reflect the high stability of the surface K–OCH_3 intermediate. The additional formation of the H_2CO reaction product reveals that surface basic sites are also capable of undergoing redox reactions.

The basic surface reaction mechanism proceeds via:

$$CH_3OH + * + O* \leftrightarrow CH_3O* + HO* \quad (11)$$

$$CH_3O* + O* \rightarrow H_3CO_2* + * \quad \text{rds : ratedeterminingstep} \quad (12)$$

$$H_3CO_2* + * \rightarrow H_2CO_2 + H* \quad (13)$$

$$H_2CO_2* + * \rightarrow HCOO* + H* \quad (14)$$

$$HCOO* + * \rightarrow CO_2 + H* + * \quad (15)$$

$$H* + O* \leftrightarrow HO* + * \quad (16)$$

$$HO* + H* \leftrightarrow H_2O + 2* \quad (17)$$

where * is the surface K site, the MARI is K–OCH_3 and the rds involves insertion of atomic oxygen into the surface methoxy intermediate to form CH_3OO* (reaction step 14). Kinetic isotope experiments with CH_3OH and CD_3OD revealed that formation of CO_x at modest conversions is independent of the specific methanol isotope [24]. This suggests that breaking of C–H bonds is not involved in the rate-determining step for CO_x formation and that oxygen insertion must be involved in the rate-determining step. The surface H_2CO_2* and HCOO* intermediates were not detected in the present investigation employing in situ Raman at 230 °C, but are well known to be the surface intermediates involved in the transformation of surface CH_3O* to CO_2 from more extensive in situ IR studies [27]. The highly stable surface K–OCH_3 intermediate is also reflected in the very low amounts of CH_3OH formed via reversible dissociative chemisoprtion of methanol, reaction step 13 (compare Fig. 3a and b).

The redox surface V–OCH_3 primarily yielded H_2CO and smaller amounts of DME. The DME is not formed from exposed Al–OCH_3 sites since they are not present in the Raman spectrum (see Fig. 2), but from surface Lewis and Bronsted acidic sites associated with the monolayer of surface VO_x on an Al_2O_3 support [19]. The redox surface mechanism proceeds via:

$$CH_3OH + * + O* \leftrightarrow CH_3O* + HO* \quad (18)$$

$$CH_3O* + * \rightarrow H_2CO + H* + * \quad \text{rds : ratedeterminingstep} \quad (19)$$

$$H* + O* \leftrightarrow HO* + * \quad (20)$$

$$HO* + H* \leftrightarrow H_2O + 2* \quad (21)$$

where * represents the surface V site, the MARI is V–OCH_3 and the rds is the scission of the C–H bond of the surface V–OCH_3 intermediate to form H_2CO at ~195 °C (see Fig. 3c). Kinetic studies with CH_3OH and CD_3OD demonstrated a significant kinetic isotope effect between these molecules, a factor of 5–6 greater for CH_3OH oxidation to H_2CO, reflecting the breaking of the C–H bond in the rate-determining step [24]. The reversible dissociative chemisorption of methanol, reaction step 20, also occurs readily on the surface VO_x sites at ~177 °C. It is interesting that the CH_3OH T_p occurs about 20 °C below the T_p for the main reaction product, which indicates the ease with which the surface CH_3O* species are able to recombine with surface H* to desorb as CH_3OH. Transient kinetic isotope studies with CH_3OH and CD_3OD further reveal that the hydroxyl H–D exchange is extremely efficient for the formation of CH_3OD and CD_3OH [23,24].

The addition of 11.5% K_2O to the supported 20% V_2O_5/Al_2O_3 catalyst markedly affects the TPSR products as well as their T_p values (see Fig. 3d). The formation of DME is completely suppressed since the basic surface KO_x has completely titrated the surface acidic sites. The primary surface site for the 11.5% K_2O/20% V_2O_5/Al_2O_3 catalyst is V with some minor exposed K sites (see Fig. 2), the MARI is V–OCH_3 and the rds is the scission of the C–H bond of the surface V–OCH_3 intermediate to form H_2CO. Thus, this catalyst follows the same redox reaction mechanism as shown above for reaction steps 18–21. The major T_p value for the formation of H_2CO is increased from 195 to 255 °C, which reflects a significant decrease in the kinetics of H_2CO formation from the surface V–OCH_3 due to the retarding influence of the surface KO_x species on the redox properties of the surface V–OCH_3 species (see Tables 2 and 3). Interestingly, the slower kinetics of the redox reaction of surface V–OCH_3 to H_2CO enhances the relative kinetics of the reversible recombination of V–OCH_3 and H* to form CH_3OH (reaction step 18) since the ratio of H_2CO/CH_3OH decreases in the TPSR experiment (see Table 2).

Addition of 20% V_2O_5 to the supported 11.5% K_2O/Al_2O_3 catalyst markedly affects the reaction products as well as the kinetics of the methanol oxidation reaction. However, the results are not completely the same as for the 11.5% K_2O addition to the supported 20% V_2O_5/Al_2O_3 catalyst discussed above. Most notably, only the surface V–OCH_3 species are present for the supported 20% V_2O_5/ 11.5% K_2O/Al_2O_3 catalyst and the T_p value occurs at a lower temperature reflecting the more active nature of the resultant surfaceV–OCH_3 species in this catalyst. The exclusive formation of 100% H_2CO redox product for this catalyst at steady state, versus 85% H_2CO and 15% CO_2 from the exposed basic surface KO_x sites for the supported 11.5% K_2O/20% V_2O_5/Al_2O_3 catalyst (see Table 3), further confirms the absence of exposed active surface KO_x sites.

The above studies demonstrated that it is possible to design the surfaces of supported metal oxide catalysts to yield 100% surface acidic sites (the Al_2O_3 support), 100% surface basic sites (11.5% K_2O/Al_2O_3), 100% surface redox sites (20% V_2O_5/11.5% K_2O/Al_2O_3) or mixed surface acidic-redox sites (20% V_2O_5/Al_2O_3) as well as surface basic-redox sites (11.5% K_2O/20% V_2O_5/Al_2O_3). Methanol oxidation over a supported 15% V_2O_5/Al_2O_3 catalyst, containing both surface acidic-redox sites, was found to yield high selectivity towards DMM at reaction temperatures of 180–190 °C where the surface concentration of CH_3O* was very close to monolayer coverage [28]. The condensation of

CH_3OH to $(CH_3O)_2CH_2$ requires (1) initial formation of H_2CO on surface redox sites, (2) subsequent reaction of H_2CO with surface methoxy species on adjacent surface acidic sites and (3) a high surface concentration of CH_3O^* species to facilitate the previous reaction step involving the reaction of H_2CO with two methanol/methoxy molecules. In contrast, only low selectivity to DMM formation could be obtained on the surface acidic Al_2O_3 support and the surface redox supported 20% V_2O_5/11.5% K_2O/Al_2O_3 catalysts.

Conclusion

In summary, the surfaces of the supported $K_2O–V_2O_5/Al_2O_3$ catalytic system could be designed to yield 100% surface acidic sites (Al_2O_3), 100% surface basic sites (K_2O/Al_2O_3), 100% surface redox sites ($V_2O_5/K_2O/Al_2O_3$), mixed surface redox-acidic sites (V_2O_5/Al_2O_3) and mixed surface redox-basic sites ($K_2O–V_2O_5/Al_2O_3$). During CH_3OH oxidation, (1) the surface acidic sites consisted of Al–OCH_3 intermediates that exclusively yielded CH_3-OCH_3, (2) the surface basic sites consisted of K–OCH_3 intermediates and primarily yielded CO_2 and minor amounts of H_2CO, (3) the surface redox sites consisted of V–OCH_3 intermediates and exclusively yielded HCHO, (4) the mixed surface redox-acidic sites consisted of V–OCH_3 intermediates and yielded HCHO and $(CH_3O)_2CH_2$, and (5) the mixed surface redox-basic sites consisted of V–OCH_3 and K–OCH_3 intermediates that yielded HCHO and CO_2, respectively. The reactivity of the different surface reaction intermediates was found to be V–OCH_3 $\sim$ Al–OCH_3 > K–OCH_3 and the reactivity of the surface V–OCH_3 could be modified by the addition of potassium oxide and its order of impregnation (before or after the impregnation of vanadia). Impregnation of Al_2O_3 by potassium oxide before vanadia addition resulted in a stronger interaction between the potassium oxide and Al_2O_3, which resulted in a more active surface VO_x species. However, impregnation of Al_2O_3 by vanadia before potassium oxide addition resulted in a stronger interaction between the vanadia and potassium oxide, which resulted in a less active surface VO_x species. Thus, the desired selectivity characteristics can be tuned by the design of the catalytically active surface sites: basic surface potassium oxide was able to suppress the activity of surface acidic sites, and redox surface vanadia sites were able to suppress the activity of the surface basic sites while still retaining their active redox properties.

Acknowledgements

This paper is dedicated to the memory of Dr. Robert Beyerlein, formerly director of catalysis at the Department of Energy-Basic Energy Sciences division. The authors gratefully acknowledge the financial support of the Department of Energy, Basic Energy Sciences (grant DEFG02-93ER14350) for this work. The authors would also like to acknowledge Professor J.-M. Jehng, Dr. Y. Chen and Mr. S. Choi for their assistance.

References

[1] I.E. Wachs, B.M. Weckhuysen, Appl. Catal. A: Gen. 157 (1997) 67.
[2] J.P. Dunn, H.G. Stenger Jr., I.E. Wachs, Wachs, Catal. Today 301 (1999) 51.
[3] C.L. Pieck, S. del Val, M. Lopez Granados, M.A. Banares, J.L.G. Fierro, Langmuir 18 (2002) 2642.
[4] M.G. Nobbenhuis, A. Baiker, P. Barnickel, A. Wokaun, Appl. Catal. A: Gen. 85 (1992) 157.
[5] T. Blasco, J.M. Lopez Nieto, Appl. Catal. A 157 (1997) 117.
[6] X.T. Gao, M.A. Banares, I.E. Wachs, J. Catal. 188 (1999) 325.
[7] A. Khodakov, B. Olthof, A.T. Bell, E. Iglesia, J. Catal. 181 (1999) 205.
[8] C.P. Kumar, K.R. Reddy, V.V. Rao, K.V.R. Chary, Green Chem. (2002) 513.
[9] G. Deo, I.E. Wachs, J. Catal. 146 (1994) 335, 323.
[10] L. Lietti, P. Forzatti, G. Ramis, G. Busca, F. Bregani, Appl. Catal. 3 (1993) 13.
[11] J.M. Lopez Nieto, P. Concepcion, A. Dejoz, F. Melo, H. Knozinger, M.I. Vasquez, Catal. Today 61 (2000) 361.
[12] D. Courcot, A. Ponchel, B. Gryzbowska, Y. Barbaux, M. Rigole, M. Guelton, J.P. Bonelle, Cat. Today 33 (1997) 109.
[13] D.A. Bulushev, E.M. McCarron, L. Kiwi-Minsker, A. Renken, Langmuir 17 (2001) 5276.
[14] G. Garcia Cortez, J.L.G. Fierro, M.A. Banares, Catal. Today 78 (2003) 219.
[15] L.J. Burcham, G. Deo, X.T. Gao, I.E. Wachs, Topics Catal. 11 (2000) 85.
[16] T. Feng, J.M. Vohs, J. Catal. 208 (2002) 301.
[17] L.E. Briand, W.E. Farneth, I.E. Wachs, Catal. Today (2000) 219.
[18] M.A. Banares, I.E. Wachs, J. Raman Spectros. 33 (2002) 359.
[19] A.M. Turek, I.E. Wachs, E. Decanio, J. Phys. Chem. 96 (1992) 5000.
[20] M.T. Xu, J.H. Lunsford, D.W. Goodman, A. Bhattacharyya, Appl. Catal. A 149 (1997) 289.
[21] J.M. Tatibouet, Appl. Catal. A: Gen. 148 (1997) 213.
[22] T. Ono, Y. Tanaka, T. Takeuchi, K. Yamamoto, J. Mol. Catal. 159 (2000) 293.
[23] W.L. Holstein, C.J. Machiels, J. Catal. 162 (1996) 118.
[24] J.M. Tatibouet, H. Lauron-Pernot, J. Mol. Catal. A:Chem. 171 (2001) 205.
[25] L.J. Burcham, M. Badlani, I.E. Wachs, J. Catal. 203 (2001) 104.
[26] H.C. Liu, P. Cheung, E. Iglesia, J. Catal. 217 (2003) 222.
[27] G. Busca, Catal. Today 27 (1996) 457.
[28] J. Tavakoli, I.E. Wachs, in press.